ELSEVIER

Earth and Planetary Science Letters 203 (2002) 937–955

EPSL

www.elsevier.com/locate/epsl

Effects of repetitive emplacement of basaltic intrusions on thermal evolution and melt generation in the crust

C. Annen *, R.S.J. Sparks

Department of Earth Sciences, University of Bristol, Wills Memorial Building, Queens Road, Bristol BS8 1RJ, UK

Received 25 February 2002; received in revised form 12 August 2002; accepted 19 August 2002

Abstract

A one-dimensional thermal conduction model simulates the repetitive intrusion of basalt sills into the deeper parts of the crust. The model assumes geothermal gradients of 10–30°C km^{-1}, and intrusion depths at 20 and 30 km. A range of intrusion rates from 50 m of intruded basalt every 1000, 10 000 and 100 000 years cover a range of geodynamic situations. There is an initial incubation period in which the basalt intrusions solidify. Generation of silicic melts initiates when the solidus temperatures of either the basalt magma or surrounding crust is reached. At an intrusion rate of 50 m per 10 000 years incubation periods in the range 10^5–10^6 years are estimated, consistent with geochronological and stratigraphic data on many volcanic systems where there is commonly an evolution from mafic to silicic volcanism. Melt generation involves simultaneous cooling and crystallization of intruding basalt and partial melting of both new basaltic crust and pre-existing old crust. The proportion of these components depends on the fertility of the crust, in particular the abundance of hydrous minerals, and the temperature and water content of the basalt magma. For a wet (2% H_2O) and cool (1100°C) basalt, melt generation can be dominated by residual liquids from basalt crystallization. For a dry (0.3% H_2O) and hot (1300°C) basalt emplaced into fertile crustal rocks, such as pelite, melt generation can be dominated by partial melting of old crust. Melt proportions and temperature vary greatly across such a deep crustal intrusion zone, resulting in geochemical diversity in magmas. Segregated melts, if mixed together during ascent or in a high-level magma chamber, will be geochemical hybrids with mantle and crustal components. Intrusion rates of 50 m per 100 000 years or less are too low for large-scale melt generation in the crust. Periods of magmatic intrusion create reverse geothermal gradients and thermal anomalies in the crust which will take several million years to decay. Such anomalous zones are predisposed to remelt if a subsequent magmatic episode initiates.

Keywords: intrusions; basalts; residual melts; anatexis; heat transfer

1. Introduction

The role of basalt in the generation of silicic magma is demonstrated by numerous observations. Geochemical data and temporal associations in individual volcanoes indicate that many intermediate and silicic magmas are closely asso-

* Corresponding author. Tel.: +44-117-954-52-43; Fax: +44-117-925-33-85.
E-mail addresses: c.j.annen@bristol.ac.uk (C. Annen), steve.sparks@bristol.ac.uk (R.S.J. Sparks).

0012-821X/02/$ – see front matter
PII: S0012-821X(02)00929-9

ciated with basalt [1]. Evidence for this intimate association comes from major tectonic settings, including arcs, rift zones, hot spots and ocean ridges with thickened crust, such as Iceland. Such associations occur in both continental and oceanic settings, although there is a pronounced tendency for silicic magma production to correlate with crustal thickness. The two principal concepts for generation of evolved magmas are differentiation of basalt and partial melting of crustal rocks. The heat and volatiles transferred from basaltic magma may be critical factors in many situations where partial melting of crust occurs [2,3]. Field, petrographic, and geochemical observations of volcanic and plutonic complexes also indicate intimate mingling of mafic and silicic magmas [4–11].

Field evidence and geophysical studies are consistent with mantle-derived basalt being emplaced into the crust at deep or intermediate level [12]. Layered rocks in the lower crust, visible on seismic profiles, have been interpreted as mafic sills [13–15]. Geobarometric and geothermic data obtained on xenoliths suggest temperature anomalies and reverse geothermal gradients in the lower crust and upper mantle [16,17]. Igneous intrusions have been identified in the deep parts of the crust from xenoliths and many geophysical studies (e.g. [18–20]). Petrological and geochemical studies demonstrate that basalt magmas commonly differentiate by crystallization and can interact with crustal rocks resulting in contamination and assimilation (e.g. [21]). An example of intrusion of the deep continental crust by mafic magma is the 10 km thick mafic complex in contact with granulite facies crustal rocks exposed in the Ivrea Zone (northern Italy) [22]. Geobarometric calculations indicate that these mafic intrusions were emplaced at 20 ± 5 km [23,24]. These authors [23,24] believe that cumulates crystallized from a small periodically refilled magma chamber are sitting at the top of the mafic body at a relatively fixed position through time.

Geological, geochronological, stratigraphic and petrological studies of volcanic complexes indicate that basalt magma is continuously fluxed into the crust over long periods of time [1,25–28]. This inference is consistent with models of continuous melt production in the mantle governed by plate motions and convective circulation in the mantle. Eruption and intrusion of magma in the crust are episodic, which can partly be attributed to the complexity of magma ascent processes through the lithosphere with stagnation of magmas at specific depths due to density effects [29], stress variations [30] or lithological discontinuities [31].

The heat transfer processes of magma intrusions have typically involved consideration of the thermal evolution of a single instantaneously emplaced intrusion (e.g. [2,32,33]). Huppert and Sparks [2] studied experimentally and analytically the melting of the roof of a convecting basaltic sill. Barboza and Bergantz [34] examined numerically the heat transfer from a semi-infinite mafic magma body below crustal rocks. Huppert and Sparks [2] showed that the intrusion of basalt can generate crustal melts rapidly in a few hundreds years. Bergantz and Dawes [35] recognized that multiple intrusions are required for regional scale magma generation. Given that mafic magma is continuously generated from the mantle, the long-term thermal evolution of crust is more likely controlled by the accumulated effects of a large number of incremental additions of magma over long time periods. Petford and Gallagher [36] investigated the effect of repetitive intrusions in a mafic lower crust on short time scales ($\sim$10 kyr) and at high magma intrusion rates. They show that multiple accretion is more efficient in heating the crust than one large single body. This paper considers the cumulative effects of successive inputs of mafic magma over tens of thousands to millions of years, and investigates different assumptions on the compositions and water contents for crust and basalt, and about the depth and spacing of basalt intrusions. With a simple and general model we investigate the simultaneous generation of evolved melt both from basalt crystallization and crustal partial melting due to repetitive intrusions of basalt into the crust over a long period of time.

2. The model

We simulate the intrusion of repetitive basaltic

injections emplaced into the crust. The geothermal gradient determines the initial temperatures before the first injection. We assume a geothermal gradient of 20°C km^{-1}. We also investigate models with geothermal gradients of 10°C km^{-1} and 30°C km^{-1}. In a first model each successive basalt is intruded at a constant depth on the top of previously intruded material. The modelled depth can be the lower crust–upper crust boundary at 20 km or the mantle–lower crust boundary at 30 km. Those are boundaries where mafic magmas might preferentially stagnate and might correspond to the neutral buoyancy level of basaltic magma [29] or a mechanical boundary [19]. For our chosen geotherm the temperature at the lower–upper crust boundary is 400°C and is therefore close to the brittle–ductile transition at typical tectonic strain rates (e.g. [37]). The temperature at the model Moho depth is 600°C. In a second model the mafic intrusions are scattered randomly over a zone in the crust and screens of crustal rocks are sandwiched between the successive intrusions. In all models, at the time of each intrusion, the whole crust below the sill is displaced downward in order to accommodate the new volume.

Partial melting depends on the presence of fluids, especially water. We modelled several upper and lower crust compositions. The main difference between the model compositions lies in the type and quantity of hydrous minerals, which control both the total water content and the temperature of extensive dehydration melting. The petrology we chose for the upper crust is a pelite and a granodiorite containing a total amount of mineral-bound water of 1.7 and 0.3% respectively. We informally describe the pelite as 'fertile' and the granodiorite as 'infertile', reflecting the much larger amounts of melt that can be generated from the pelite at a given temperature. The lower crust is either an amphibolite with a total amount of 0.6% water or a dry mafic granulite. Again the amphibolite is referred to as 'fertile' and the granulite as 'infertile'. As shown by experimental work [38–40], the melt fraction can be sensitive to the mode of the rock. Thus our 'fertile' and 'infertile' compositions represent two end members of crustal melt production. The magma invading the crust was modelled to represent a range of common basalts from relatively dry high-temperature magma, as might be generated in a hot spot, to cool relatively wet magma, as can be generated in arcs. Our choice of parameters is dry basalt at 1300°C containing 0.3% water and cooler basalt at 1100°C with 2% water. We assume that the water contained in the basalt does not escape into the crust. However, in nature, water released by solidifying basalt might flux into overlying heated crust and promote melting, and deserves future consideration.

We use a finite difference method to compute the conductive heat transfer from each intrusion into the crust. The model is static with generated melt and any excess fluid remaining in situ. There will be many complex dynamical processes within such a deep crustal hot zone, including localized assimilation of surrounding rocks by individual intrusions [21], enhanced rates of local heat transfer by convection [2], melt segregation by compaction [41] and deformation [42], and perhaps large-scale buoyancy instabilities caused by high temperatures and melt generation in the growing intrusion zone [43]. Additionally, when melt proportions exceed about 20–25%, then the system is better described as magma than partially molten rock and magma convection may become important [44]. We argue that all these dynamical processes do not have large effects on the large-scale heat sharing and melting relationships captured in a conductive heat transfer model [35]. For example simultaneous segregation and ascent of partial melts does not affect significantly the overall thermal balances, although an alternative model in which melt is immediately removed will have a detailed influence on the total amount of melt generated and melt compositions.

The crust domain is divided into an array of cells. A rock composition, a temperature and a melt fraction are attributed to each cell. Temperature and melt fraction are computed using the finite difference expression of the conductive equation of heat balance:

$$\varrho C_{\mathrm{p}}\frac{\partial T}{\partial t}+\frac{\partial X}{\partial t}\varrho L=k\frac{\partial^2 T}{\partial x^2} \quad (1)$$

ϱ is density, C_{p} is specific heat capacity, T is tem-

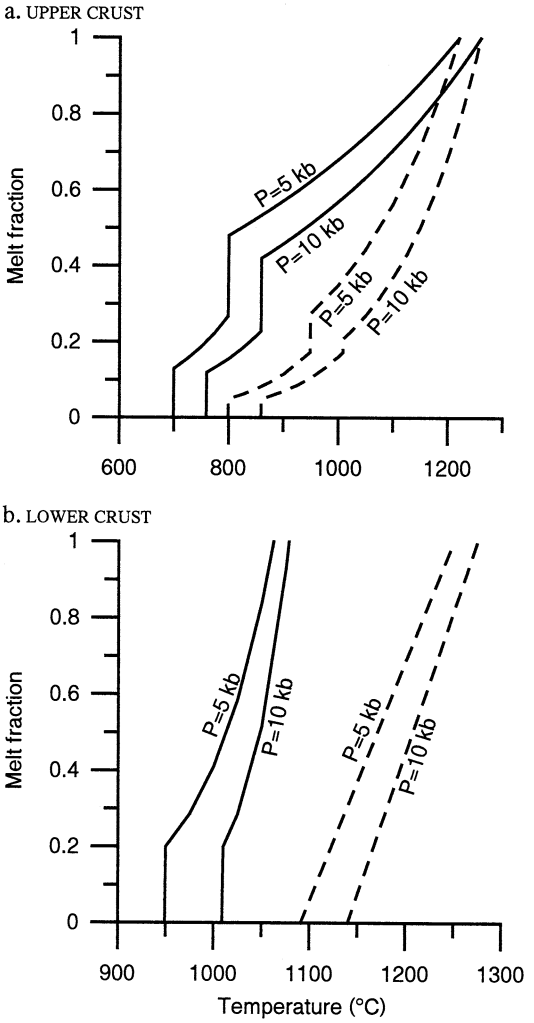

Fig. 1. Melt fraction curves for upper crust and lower crust lithologies after [33,45–49]. Examples given for 5 and 10 kbar pressure. (a) Plain lines: pelite with 20% muscovite, 20% biotite, 1.7% of total water; dashed lines: granodiorite with 5% biotite, 5% amphibole, 0.3% total water. (b) Plain lines: amphibolite with 30% amphibole, 0.6% water; dashed lines: dry mafic granulite.

perature, t is time, X is melt fraction, L is latent heat of fusion, k is thermal conductivity and x is distance.

The melt fraction between solidus and liquidus depends on temperature and mineralogy. We have parameterized these relationships based on experimental studies. Except for dry granulite, the crustal rocks in our model are subject to dehydration melting. The solidus coincides with the breakdown temperature of the first hydrous mineral. The amount of melt produced at the breakdown temperature of a hydrous mineral depends on the total amount of water fixed in this mineral and is given by Clemens and Vielzeuf [45] at 5 and 10 kbar. If a second hydrous mineral is present, as in pelite and granodiorite, the melt fraction at the breakdown temperature of the second mineral can similarly be estimated [45]. The solidus and liquidus of the rocks and the breakdown temperatures of muscovite, biotite and amphibole were compiled from [33,45–49]. The amount of melt produced at the breakdown temperature of hydrous minerals at pressures different from 5 and 10 kbar is linearly interpolated. The melting degree between the breakdown temperature of the two hydrous minerals, and between the last hydrous mineral and the liquidus is exponentially interpolated. Figs. 1 and 2 show melting curves for 5 and 10 kbar pressures which we have parameterized. For the dry granulite we assume a linear melt–temperature relation between the solidus and the liquidus (Fig. 1b). For the dry hot basalt we have adopted a strongly curved melting relation (Fig. 2), which allows most of the crystallization to occur at high temperature, but takes

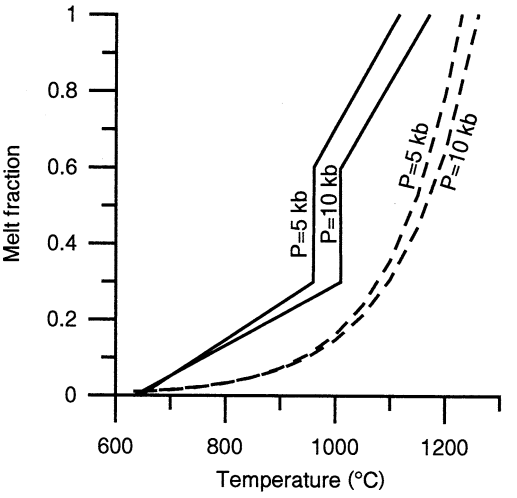

Fig. 2. Melt fraction curves compiled from [33,46–49] for wet cool basalt with 2% water (plain lines) and dry hot basalt with 0.3% water (dashed lines). Examples given for 5 and 10 kbar pressure.

Table 1
Main physical property values used in model calculations

					Reference
ϱ	density	injected basalt	2800	kg m^{-3}	[3,33,69]
		upper crust	2650		[12]
		lower crust	3050		[12]
C_p	specific heat capacity	injected basalt	1480	J kg^{-1}	[33,68]
		upper crust	1370		[68]
		lower crust	1390		[68]
L	specific latent heat	injected basalt	4.0×10^5	J kg^{-1} K^{-1}	[2,68]
		upper crust	2.7×10^5		[68]
		lower crust	3.5×10^5		[68]
k_0	thermal conductivity at surface temperature and pressure	injected basalt	2.6	J s^{-1} m^{-1} K^{-1}	[50]
		upper crust	3.0		[50]
		lower crust	2.6		[50]

Sources are given by numbers.

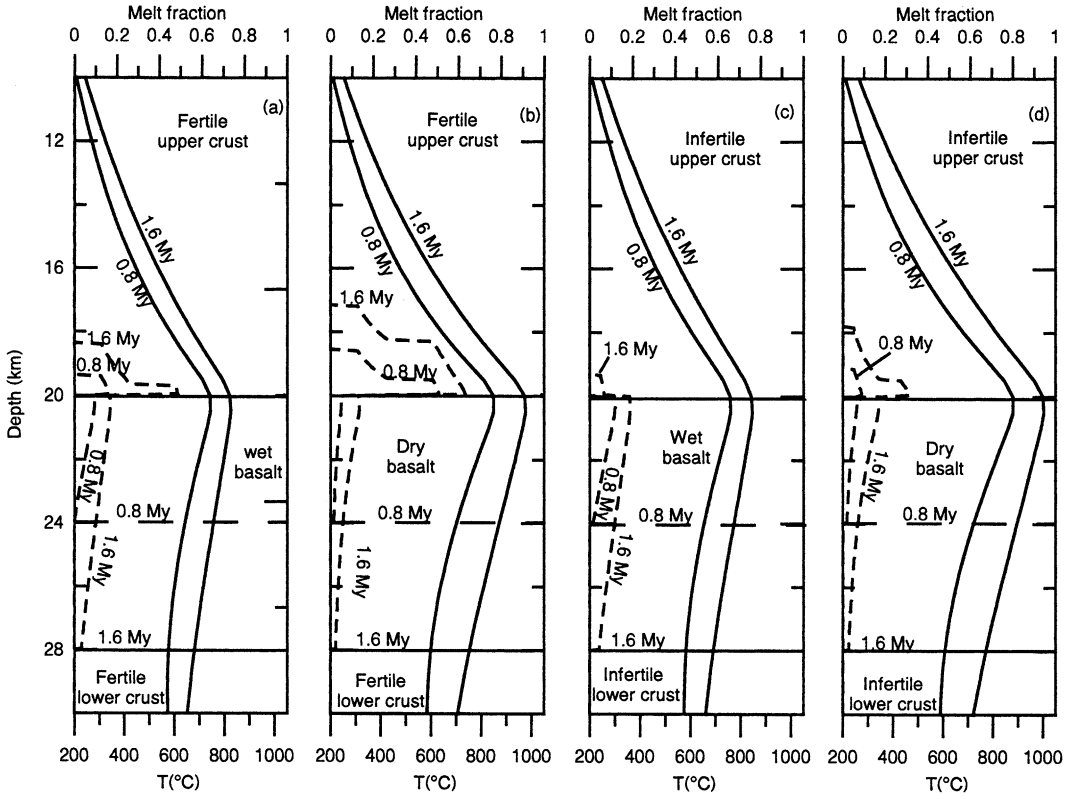

Fig. 3. Profiles of temperature (plain lines) and melt fraction (dashed lines) in the crust after 0.8 Myr and 1.6 Myr due to intrusion of 50 m thick sills every 10 000 years. (a) The upper crust is pelitic and the basalt is injected at 1100°C with 2% water. (b) The upper crust is pelitic, the basalt is injected at 1300°C with 0.3% water. (c) The upper crust is granodioritic, the basalt is injected at 1100°C with 2% water. (d) The upper crust is granodioritic, the basalt is injected at 1300°C with 0.3% water.

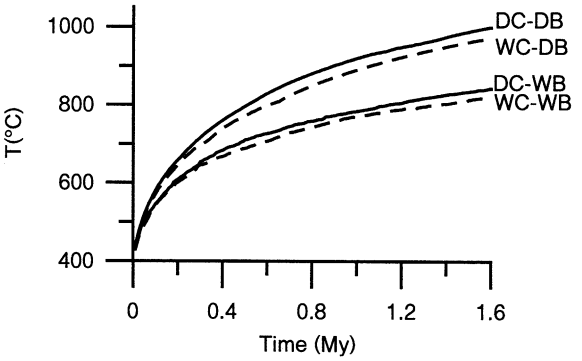

Fig. 4. Evolution of the temperature with time at the boundary between intrusion and upper crust. A 50 m thick sill is intruded every 10 000 years. WB: wet basalt (1100°C, 2% water). DB: dry basalt (1300°C, 0.3% water). WC or dashed lines: fertile upper crust (pelitic). DC or plain lines: dry upper crust (granodioritic).

account of the concentration of water in residual melt so that the solidus is at the wet granite melting curve. The crystallization curve of the wet basalt is stepwise because it crystallizes amphibole, and has a solidus temperature at the wet granite solidus (Fig. 2).

An estimate of the length W affected by the heat loss at the system boundary after a time t is given by:

$$W \approx \sqrt{\varkappa t} \tag{2}$$

κ is thermal diffusivity. The horizontal heat loss at the extremities of the sills does not affect the temperature distribution of the system if the duration of the intrusion is kept sufficiently short. If we assume a sill horizontal extension of 20 km, $\kappa = 7\times10^{-7}$ m^2 s^{-1} and keep the duration less than 4 Myr, then a one-dimensional model is reasonable.

The parameters used in the model are reported in Table 1. The conductivity depends upon temperature and pressure as described by Chapman and Furlong [50].

Magma production rates are estimated from volcanic output rates and assumptions about the ratio of intrusive to extrusive products [25,51,52]. Crisp [51] estimated from a global study an intrusive to extrusive ratio ranging from 5:1 to 10:1. However, recent works [53,54] show that the thickness of sheet tabular intrusions may have been overestimated in Crisp's study. In order to estimate rates of intrusion in a one-dimensional model an additional assumption is required about the intrusion area for a given magma flux. Volcanic output rates are typically in the range 10^{-2} to 10^{-4} km^3/year [25]. Estimates for output rates in arcs are typically 10–30 km^3/km/year [25] with rates of individual arc volcanoes being 3×10^{-4} to 3×10^{-3} km^3/year. Here a value of 2×10^{-3} km^3/year is chosen as the intrusion rate, assuming that the ratio of intrusive to extrusive igneous rocks is 2 and that 10^{-3} km^3/year is representative of volcanic output rates. We further assume that this magma is intruded over an area of 20×20 km to yield a representative intrusion rate of 50 m per 10 000 years. We also carried out calculations for one order of magnitude higher and lower than this representative value. Notwithstanding considerable uncertainty about the ratio of extrusion to intrusion and the appropriate area to take, model calculations spanning three orders of magnitude magma intrusion rates should cover ranges expected in most magmatic systems. Petford and Gallagher [36] modelled intrusion rates at the upper end of the spectrum considered here with their representative rate higher than our highest rate. Their representative rate is likely to be most applicable to volcanic systems with very high magma production rates, comparable to Hawaii,

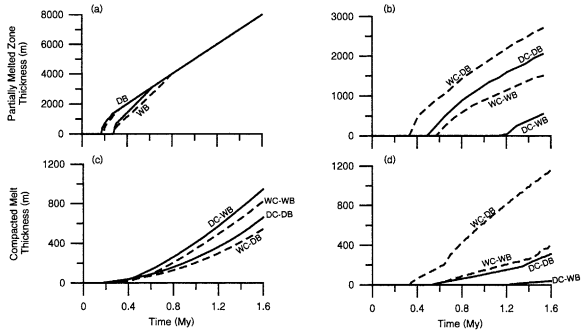

Fig. 5. Thickness variation with time of the partially melted zone of newly intruded basalt (a) and upper crust (b) and equivalent compacted melt thickness of intruded basalt (c) and upper crust (d). WB: wet basalt (1100°C, 2% water). DB: dry basalt (1300°C, 0.3% water). WC or dashed lines: fertile upper crust (pelitic). DC or plain lines: dry upper crust (granodioritic).

and to short transient periods with rates well above the average in most volcanic systems.

3. Results

Here we use the following terminology. The growing layer of basalt is described as new crust to distinguish it from the pre-existing old crust. We use the term partial melt in a sense that does not distinguish between partial melting of pre-existing rocks and residual differentiated melts derived from cooling and crystallization of newly emplaced basalt intrusions. Implicit in the model is that both partial melting of new basalt crust and old crust occurs simultaneously with generation of residual evolved melts by cooling and crystallization of the basalt. The calculated amount of partial melt is reported as both an equivalent thickness of pure melt (compacted thickness) and as the thickness of partially melted rocks. The compacted thickness represents the integration of the melting degree over the partially melted layer, following McKenzie [41]. Note that we did not model the dynamic process of compaction and the compacted thickness is merely a measure of melt production.

3.1. Sills emplaced at a fixed depth

Fig. 3 shows profiles of temperature and melt proportions of the crust induced by the injection of a 50 m thick sill every 10 000 years at 20 km depth for a total duration of 1.6 Myr. At that time the upper and lower crust are separated by 8 km of newly intruded basalt. A temperature anomaly develops at the depth where sills are injected, with a reverse geotherm below the zone of intrusion (Fig. 3). Fig. 4 shows the evolution of temperature with time at the intrusion–upper crust boundary. There is an incubation period while the temperature builds up in the intrusion zone before extensive melt production starts (Fig. 5). Each intrusion cools to the surrounding temperature on a time scale much shorter than the interval between intrusions and so in the incubation period the basalt completely solidifies. Eventually the temperature builds up to the point when the solidus is exceeded and then a zone of partially melted rock develops and thickens with time. The partial melt is generated both as residual melt produced by crystallization of freshly injected basalt and by partial melting within the old pre-existing upper crust (Fig. 5). The incubation time before melt accumulation depends on the composition and water content of the invading basalt and crust. The incubation period before new basalt injection starts to accumulate residual melt varies between 170 kyr (dry basalt) and 300 kyr (wet basalt) (Fig. 5a, c). The time needed for the solidus temperature of the upper crust to be exceeded lies between 340 kyr (pelitic crust) and 1.2 Myr (granodioritic crust) (Fig. 5b, d). The new basalt crust is always the first to start accumulating residual melt (Fig. 5). The preferential generation of melt in the new basalt crust reflects the fact that heat is concentrated in the zone of intrusion. Heat is advected into the crustal intrusion zone faster than it can be conducted away. Melt generation in the new basaltic crust also reflects the assumption that its solidus is lower than the pelitic or granodioritic crust.

The new basalt crust has a lower melting degree than the upper crust, but a greater thickness of partially melted rock is generated. The maximum in melt fraction after 1.6 Myr lies between 14% for a dry basalt injected in a pelitic crust and 19% for a wet basalt injected in a dry crust (Fig. 3). As expected, the upper crust maximum melting degree is high for a pelitic composition (between 48 and 63%) and lower for a granodiorite composition (between 18 and 30%), depending on the basalt temperature (Fig. 3). The compacted melt thickness originating as residual differentiated melt from the basalt intrusions is almost always higher than the compacted melt thickness derived by partial melting of the upper crust (Fig. 5c, d). The exception is when a fertile upper crust is in contact with hot, dry basalt injected at 1300°C. In this case the compacted melt thickness after 1.6 Myr derived from the upper crust and from the basalt can reach respectively 1150 and 540 m.

The emplacement of the basalt at 30 km (the model Moho) is far less favorable to the melting of the old crust. An amphibolitic lower crust needs 0.87 Myr to start melting when intruded

by hot and dry basalt magma (Fig. 6) and a granulitic crust does not melt at all for 1.6 Myr duration. The initial temperature is close to the solidus of the injected magma, and thus the intruded basalt starts to accumulate residual differentiated melt after only 10 000 years. After 1.6 Myr the compacted melt thickness derived from the basalt reaches 1400 m. The maximum melting degree is 23% for the arc basalt and 30% for the dry basalt.

There are two alternative assumptions about the fate of the water contained in the basalt. First, the water stays in situ and is available for basalt remelting at its wet solidus temperature. Alternatively all excess water not incorporated into hydrous minerals during crystallization escapes during the incubation stage. In this case no basalt remelting is possible below amphibole breakdown temperature. However, once the wet solidus is reached further intrusions will contain residual melt with the water retained in solution due to high pressure. We calculate that if the water escapes after crystallization slightly less melt is produced from newly intruded crust, but nevertheless melt production remains high. After 1.6 Myr, crustal temperature, when intruded by wet basalt, does not reach amphibole breakdown temperature (Figs. 4 and 7a). Thus early solidified intrusions are not remelted if water has escaped. The difference in compacted melt thickness from basaltic crust that retains water after freezing and from basaltic crust that looses its water is only 10% (Fig. 7) for the wet case and 4% for the dry case. Most melt that accumulates in the new crust is residual from crystallization of the intrusions with remelting of formerly frozen basalt contributing minor proportions of the total melt generated even when all water is retained.

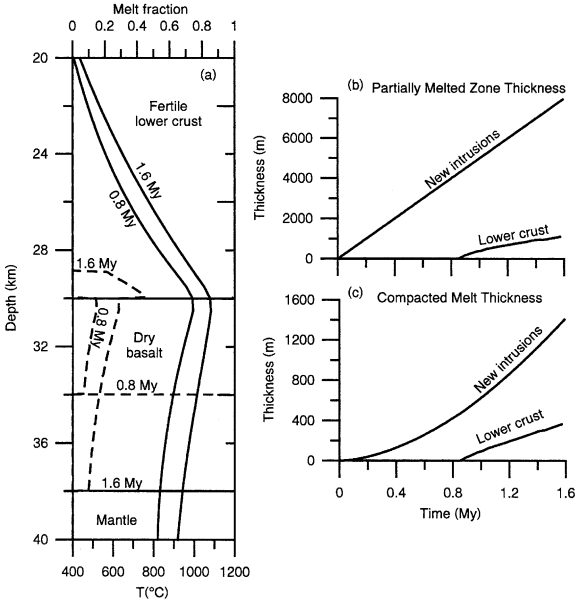

Fig. 6. Intrusion of 50 m thick sills every 10 000 years of dry basalt at the boundary between the mantle and amphibolitic lower crust. (a) Temperature (plain lines) and melt fraction (dashed lines) in the crust after 0.8 Myr and 1.6 Myr. (b) Thickness variation with time of the partially melted zone of newly intruded basalt and lower crust. (c) Equivalent compacted melt thickness variation with time of intruded basalt and lower crust.

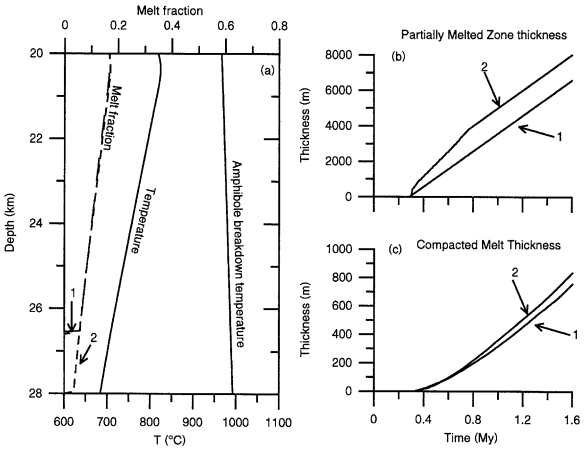

Fig. 7. Intrusion of 50 m thick sills every 10 000 years of wet basalt at the boundary between a pelitic upper crust and an amphibolitic lower crust. Curve 1 is for wet basalt that loses its water after crystallization. Curve 2 is for wet basalt that retains water after crystallization. (a) Profiles of melt fraction (dashed line) and temperature (plain line) in the new basaltic crust. Melt fraction curve 1 and curve 2 overlap between 20 km and 25.6 km depth. Basalt that retains water after crystallization is additionally melted on 1.5 more km. (b) Thickness variation with time of the partially melted zone of new crust. (c) Equivalent compacted melt thickness variation with time of new basaltic crust.

3.2. Thickness of the sills

We kept the mean magma intrusion rate constant and investigated changes in sill thickness

and injection frequency. We ran the simulations with 10, 50 and 500 m sill injected with a respective frequency of 2000, 10 000 and 100 000 years. For all tests duration is 1.6 Myr and the total thickness of intruded basalt is 8 km. We compared the results with the emplacement of a single 8 km body. The thermal evolution is only weakly sensitive to intrusion thickness and frequency for the same time-averaged magma supply rate (Fig. 8). The injection of 500 m thick sills generates a slightly lower and broader thermal anomaly than 50 m sills, but results for 10 and 50 m sills are similar. Modelling of a continuous steady basalt flux is captured by a large number of discrete small intrusions. The crust intruded by infrequent large sills is affected by cycles of crystallization and melting while more regular steady melt generation is related to frequent thin intrusions. Long-term melt generation is the same (Fig. 8b and c). Sill thickness is unimportant, because the

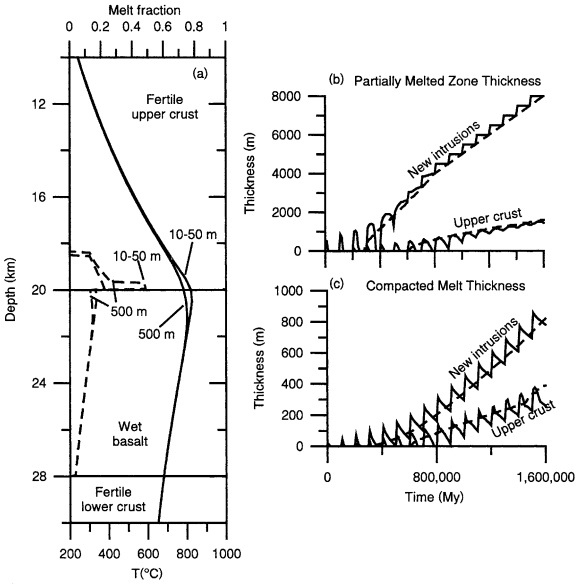

Fig. 8. Intrusion of 10, 50 and 500 m thick sills of wet basalt at the boundary between a pelitic upper crust and an amphibolitic lower crust. (a) Profiles of temperature (plain lines) and melt fraction (dashed lines) in the crust after 1.6 Myr. (b) Thickness variation with time of partially melted zone of newly intruded basalt and fertile upper crust. (c) Equivalent compacted melt thickness variation with time of intruded basalt and fertile upper crust. For (b) and (c): dashed line: 10 and 50 m thick sills; plain line: 500 m thick sills. Curves of 10 and 50 m sills overlap and cannot be distinguished.

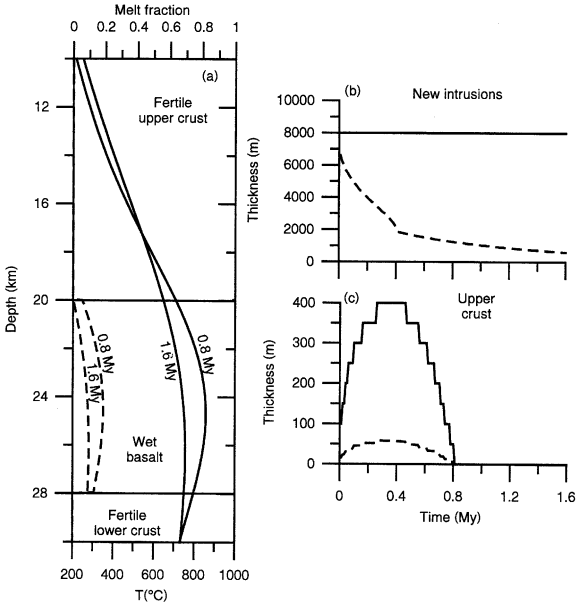

Fig. 9. Instantaneous emplacement of an 8 km basaltic body. (a) Profiles of temperature (plain lines) and melt fraction (dashed lines) in the crust after 0.8 Myr and 1.6 Myr. (b) and (c) Thickness variation with time of melted zone (plain line) and equivalent compacted melt thickness variation with time (dashed lines) of intruded basalt (b) and fertile upper crust (c).

characteristic cooling time of the sills [36] is at least one order of magnitude smaller than the time interval between intrusions.

Instantaneous emplacement of an 8 km body results 1.6 Myr after emplacement in a cooler basaltic layer and upper crust and a warmer lower crust compared with repetitive intrusion (Fig. 9a). For the single intrusion, the bulk crustal temperature does not increase with time with the fixed heat content of the sill being diffused through the crust. Melting of the upper crust reaches a maximum after some hundred thousands years (60 m of compacted melt in 300 kyr and 400 m in 700 kyr for wet and dry basalt respectively) and thereafter solidification occurs. Small basalt injections are more efficient in melting the crust than a single intrusion.

3.3. Scattered sills

An alternative model involves emplacement of

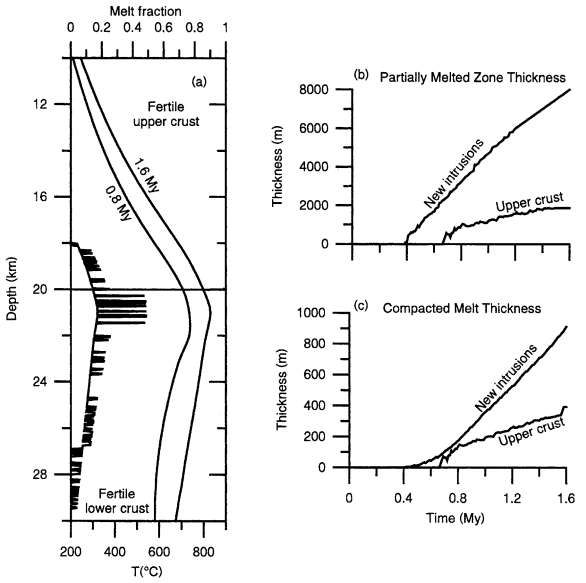

Fig. 10. Intrusion of 50 m thick sills of wet basalt every 10 000 years randomly scattered in the crust between 18 and 22 km depth. The upper crust is pelite and the lower crust is amphibolite. (a) Profiles of temperature after 0.8 Myr and 1.6 Myr and melt fraction in the crust after 1.6 Myr (the melt fraction at 0.8 Myr is not given for reason of clarity). The base line on the melting fraction profile represents the melt fraction in the randomly emplaced sills and horizontal spikes represent the melt fraction in screens of old fertile crust. (b) Thickness variation with time of partially melted zone of newly intruded basalt and upper crust. (c) Equivalent compacted melt thickness variation with time of intruded basalt and upper crust.

scattered sills. Fig. 10 shows the temperature and melting profiles and time evolution of 160 sills 50 m thick randomly emplaced over 1.6 Myr in the upper and lower crust between 18 and 22 km depth. The melt fraction profile shows intercalation of low and higher melt fractions corresponding to the alternation of basalt and crust. Upper crust and intruded basalt experience cycles of melting and solidification for a few tens kyr before extensive melt generation starts. Compared with fixed depth intrusions, the incubation time is significantly longer due to heating layers of intercalated crust. For wet basalt the melt fractions and thickness of the melted zone are similar to the case of fixed depth intrusions. For dry basalt, less melt is produced with scattered sills.

3.4. Magma intrusion rate

Calculations have been made with magma intrusion rates one order of magnitude higher and one order of magnitude lower than described above. A high magma intrusion rate (50 m sill every 1000 years) generates rapid extensive melt generation. The temperature peak is higher and narrower than with a lower rate as less time is available for heat transfer into the crust and for the cooling of intrusions between injections (Fig. 11). The incubation period for melting fertile pelitic upper crust is less than 10 000 years. The maximum melting degree is high (about 70% after 160 kyr) for both fresh and old crust. The high melting degree of the old crust is counterbalanced by a small thickness of the melted zone. After the intrusion of 160 sills, the compacted melt thickness of the old crust is only slightly greater than with a

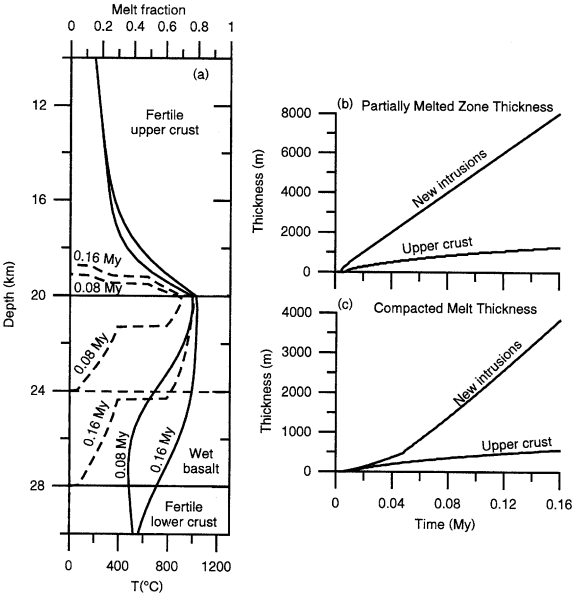

Fig. 11. Intrusion of 50 m thick sills every 1000 years of wet basalt at the boundary between a pelitic upper crust and an amphibolitic lower crust. 160 sills are injected over 0.16 Myr. (a) Profiles of temperature (plain lines) and melt fraction (dashed lines) in the crust after 0.08 Myr and 0.16 Myr. (b) Thickness variation with time of the partially melted zone of newly intruded basalt and upper crust. (c) Equivalent compacted melt thickness variation with time of intruded basalt and upper crust.

lower magma intrusion rate whereas the compacted thickness of residual melt from basalt crystallization is four times higher than with the lower intrusion rate of 50 m every 10 000 years.

For a 50 m sill every 100 000 years the heat input from the magma scarcely compensates the conductive heat loss between two intrusions. The crust heats up extremely slowly. If sills are emplaced at the upper crust–lower crust boundary, 12.7 Myr are required before a very small quantity of residual melt appears deep in the basaltic intrusions (Figs. 12a and 13) and no melting of old crust occurs. This time is an overestimate because with a 20×20 km intrusion area the system loses heat at its boundary after 4 Myr. Intrusions need to be injected at Moho depth or more where surrounding rock is hotter for significant melt generation (Figs. 12b, c and 13). Low magma intrusion rate favors generation of high pressure differentiated melts from intruding basalts. For a 20°C km^{-1} geothermal gradient the initial temperature at 40 km depth is 800°C and so here the basalt cannot completely solidify. Melt accumulation starts immediately (Fig. 13). More melt is produced at depth because higher temperature implies a higher melting degree (Fig. 13b).

3.5. Cooling of the crust

The intrusion of basalt induces a high-temperature anomaly in the crust. After basalt input has ceased the conductive heat flux is initially high within the crust and the temperature peak rapidly flattens (Fig. 14a). Decay of the anomaly then slows down (Fig. 14a, b). For the case of 8 km of basalt intruded over 1.6 Myr, 5 Myr after injections have ceased a 4.6 km thick zone of intruded basalt is still slightly above the solidus if the basalt was injected at 1300°C and only 700 m if injected at 1100°C (Fig. 14c). This corresponds to respectively 65 and 3 m of compacted melt (Fig. 14d). The crust has a long memory of thermal perturbations caused by magmatic episodes. If new episodes of magmatism begin before the

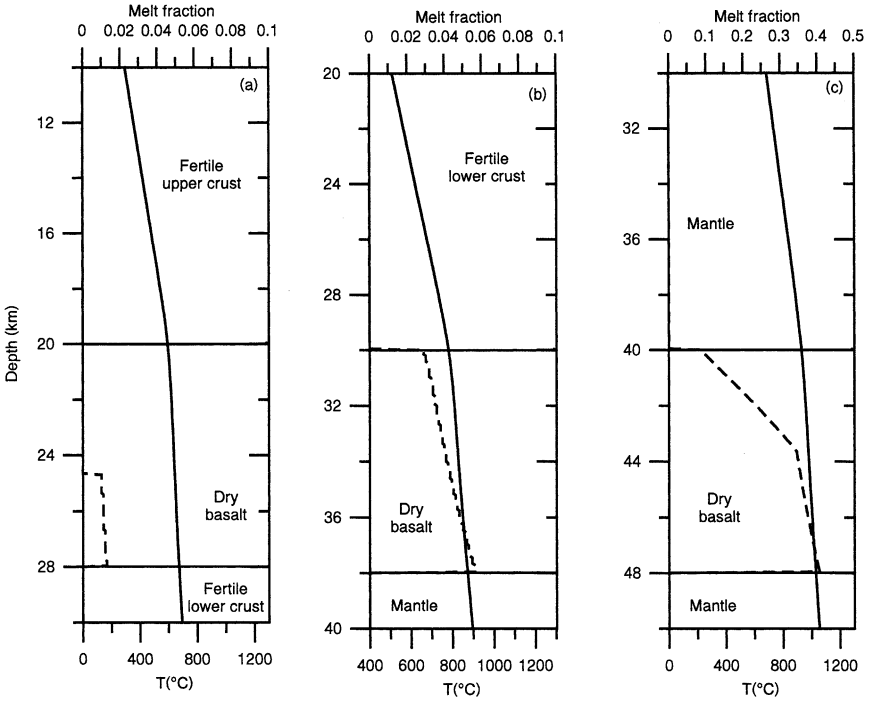

Fig. 12. Intrusion of 50 m thick sills every 100 000 years of dry basalt. Profiles of temperature (plain lines) and melt fraction (dashed lines) after 16 Myr. (a) Intrusion at 20 km at lower–upper crust boundary. (b) Intrusion at 30 km at lower crust–mantle boundary. (c) Intrusion at 40 km depth in the mantle.

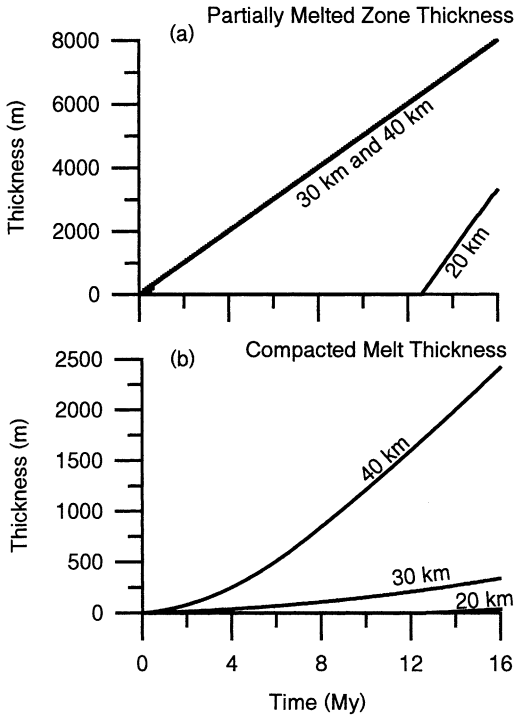

Fig. 13. Thickness variation with time of the partially melted zone (a) and equivalent compacted melt thickness variation with time (b) of intruded dry basalt injected at the low intrusion rate of one 50 m sill every 100 000 years at 20, 30 and 40 km depth.

anomaly has fully decayed then the earlier magmatic intrusions may be preferentially remelted.

3.6. The geotherm

Fig. 15 shows results for 10°C km^{-1} and 30°C km^{-1} geotherms. With high initial temperature of the crust the incubation period is reduced and more melt is produced from the new basalt crust and from old crust. However the respective contribution of each source of melt is not influenced by the initial geothermal gradient (Fig. 15).

4. Discussion

The intrusion of basalt into the crust instantaneously or periodically on time scales of less than a few thousands years does not lead to extensive crustal melting [34,36]. In contrast, our model shows that a few hundreds to more than 1 km of compacted evolved melt can be generated when basalt repeatedly invades the crust over periods of 10^5 to over 10^6 years. Two major differences between our model and the model of Petford and Gallagher [36] explain why the amount of melt the crust generated is so different. The first difference is the crust solidus temperature. The rock surrounding the intrusions simulated by Petford and Gallagher [36] is an amphibolite with a solidus close to 800°C. In contrast, the main source of melt in some of our simulations is either the pelitic upper crust with a solidus around 700°C or a wet basalt with solidus around 640°C. The second difference is that our model includes melt generated by crystallization of the invading basalt, and in most simulations this residual melt is substantial or dominant component of melt production. The third difference between the models is the time scale. In our model magma input is sustained during hundreds of thousands of years even though our time-averaged magma intrusion rates are much lower. The heat has time to diffuse to large distance while temperature slowly builds up. Thus a long incubation period precedes extensive melting. In the Petford and Gallagher model the time scale considered is short (10 000 years), but the magma intrusion rates are higher than we assumed. Consequently the melting is rapid compared to our results and melting of surrounding old crust is small.

Magma intrusion rate has a strong influence on the melting degree and melt compositions. Different magma intrusion rates can lead to similar compacted thickness of melt derived from the upper crust, but higher intrusion rates generate higher degrees of melting. Although we have not explicitly modelled melt compositions, in general we can expect that melts will be in the silicic andesite to rhyolite range based on the experimental studies of natural rocks and magmas [55–57]. The degree of partial melting varies considerably in both space (depth) and time. Thus the process simultaneously generates a wide range of melt compositions. From this we conclude that deep crustal intrusion zones may be where much of the geochemical diversity of magmas originates.

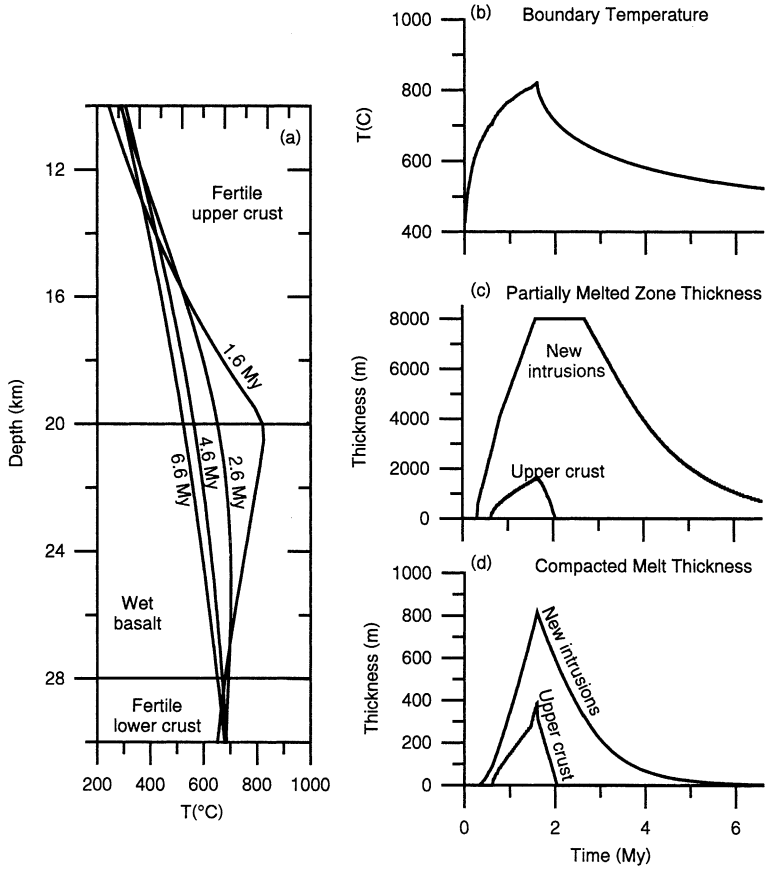

Fig. 14. (a) Temperature evolution with time after the intrusion of 160 sills during 1.6 Myr followed by a repose period of 5 Myr. Temperature profiles at 1.6 Myr, 2.6 Myr, 3.6 Myr and 5.6 Myr corresponding respectively to the end of the magmatic event, 1 Myr, 3 Myr and 5 Myr of repose. (b) Evolution of temperature with time at the intrusion–upper crust boundary. (c) Thickness variation with time of the partially melted zone of newly intruded basalt and upper crust. (d) Equivalent compacted melt thickness variation with time of intruded basalt and upper crust.

In most cases the new intrusions are the main source of partial melt due to crystallization. In the case of wet basalts the newly intruded igneous material is dominant. The contribution of the old crust may be minimal for anhydrous mafic lower crust, limited for granodiorite upper crust and still subordinate even for fertile crustal rocks such as pelite. Dry basalt intrusions generate less melt, but are high temperature and so can cause melting of older crust on a kilometric scale if the crust is fertile (e.g. pelite).

The two main concepts for generation of evolved melt in the crust are differentiation of basalt and partial melting of the crust. These processes can occur together when each increment of magma addition results in differentiation of the basaltic input forming residual melts and partial melting of old pre-existing crust with possible remelting of formerly intruded basalt. A mantle origin isotopic signature for granites and rhyolites is common (for example [52,58–60]). Studies by De Paolo et al. [61] on Sr and Nd isotopes of Late Cretaceous to Pleistocene granitic rocks and large volume rhyolites of the western USA indicate that silicic magmas form both by crustal anatexis and mantle melting or with subequal amounts of those two components. Silicic melt generation derived from recently injected basalt explains the occur-

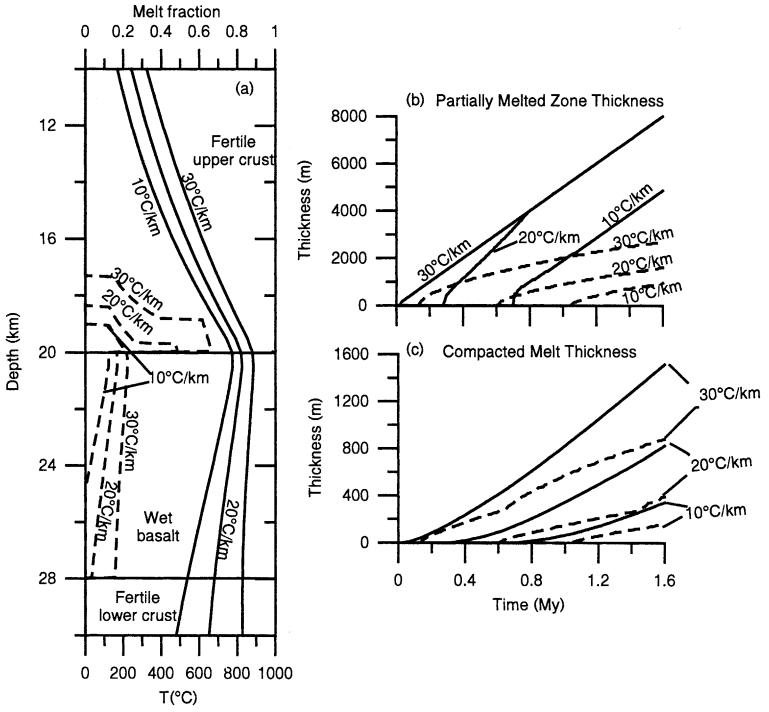

Fig. 15. Intrusions of 50 m thick sills every 10 000 years of wet basalt in a fertile crust for geotherms of 10°C km^{-1}, 20°C km^{-1} and 30°C km^{-1}. (a) Profiles of temperature (plain lines) and melt fraction (dashed lines) after 1.6 Myr. (b) Thickness variation with time of the partially melted zone of newly intruded basalt (plain lines) and upper crust (dashed lines). (c) Equivalent compacted melt thickness of intruded basalt (plain lines) and upper crust (dashed lines).

rence of granites and rhyolitic volcanics with mantle isotopic signatures, as well as the observation that intermediate to silicic magmas commonly lie on isotopic mixing arrays between mantle and crust.

As already shown by Petford and Gallagher [36] the partial melting of a mafic lower crust produces less melt compared to the partial melting of a pelitic crust. Our model shows that melt derived from basalt crystallization can be produced at any intrusion depth but in larger quantity if the sills intrude at the Moho where the surroundings are already hot. In models of underplating it is commonly assumed that the basalt is injected at Moho level around 30 km. However, geobarometric studies of the xenoliths of east Eifel volcanic field [19] suggest that mafic magma might accumulate at a depth of 20 ± 5 km. Another example of the presence of melt at this level is the Socorro magma body in New Mexico. The estimated depth of the Socorro body roof is 19 km and seismic data suggest partially molten roots extending several kilometers downward [62]. The melting of the old crust is greatly enhanced if basalt is in contact with a fertile upper crust. Basalt at 1300°C intruded below a pelitic upper crust at 20 km depth during 1.6 Myr can generate up to 1150 m of melt by partial melting of the upper crust. Thus this level should be a favorable place for the generation of silicic melts with crustal signature. The hypothesis of upper crust as a preferential source for old crust-derived melt is corroborated by De Paolo et al. [61] who concluded from isotopic data that granitic magmas, when melted from continental crust, are typically melted from intermediate to silicic source rocks and not from mafic source rocks.

An incubation period precedes the onset of extensive melt generation. One theory for infrequent eruptions of large volumes of evolved melt is the

slow differentiation of mafic magma in a large shallow magma chamber [25]. Our model suggests an alternative explanation of silicic melt production by intrusion of basalt deep in the crust. For a magma intrusion rate of 50 m per 10 000 years at 20 km depth, the crust heats up over a few hundreds of thousands of years. During this time some of the basalt is still able to reach the surface. Eventually the solidus temperature at depth of the basalt and of the surrounding crust is exceeded and evolved melt is produced by crystallization of the basalt and anatexis of the crust. The rapidity of onset of silicic melt generation may be even greater due to basalt magma being trapped. Prior to the onset of melting some basalt can escape to the surface so that the intrusion rate at depth is reduced compared to the overall magma flux. Once melting starts basalt may be prevented from reaching the surface so that the *effective* magma intrusion rate increases. This hypothesis is supported by the observation that many continental volcanoes evolve in time from erupting mafic magmas to highly differentiated silicic products. For example, in the western USA, highly silicic ash flow emission and associated caldera collapse took place after prolonged intermediate composition volcanic activity [26]. Lead and strontium isotopic ratio of rhyolitic–basaltic association at Yellowstone are interpreted by Doe et al. [63] as indicators that large mafic intrusions were injected into the lower crust resulting in rhyolite generation. At Long Valley, California basaltic volcanism began at about 3.2 Myr [27]. At 2.1 Myr there was a marked change with generation of large volumes of rhyolitic magma, which from then on dominated surface volcanic products [64]. Such sequences are consistent with accumulation of basaltic intrusions in the deep crust, culminating with the onset of melting and silicic magma generation and the entrapment of basalt deep in the crust thereafter.

At Santorini Druitt et al. [28] recognized two major cycles, each of about 200 kyr length, in which prolonged mafic to intermediate volcanism culminates in large silicic eruptions of tens of km^3 in volume and caldera formation. The silicic eruptions are preceded by long periods of dormancy ($\sim$30 kyr). Such sequences can be interpreted in terms of a steady flux of basaltic magma that is partly extruded and partly intruded. Eventually enough magma is intruded at depth to generate a significant zone of melting, trapping ascending basalt and preventing surface activity. This promotes generation of large volumes of silicic melt in the deep crust by the mechanisms modelled in this paper. Eventually the silicic melt segregates, rises to form a large shallow chamber and eventually erupts. Such a model is consistent with the study of Cottrel et al. [65] on Santorini silicic magmas where they interpreted the petrology, in the context of experimental data, as due to ascent of large volumes of silicic magma from a deeper source into a shallow chamber prior to eruption.

Our model is static and conductive. However, a deep crustal intrusion zone is likely to be dynamic. This is self-evident in volcanic systems where magmas have resided in the crust for sufficient time intervals for differentiation and partial melting to take place, but episodically ascend and erupt. Once a deep melt zone has initiated then there is generation of buoyancy and possibly overpressures related to melting [66]. Furthermore there will be tectonic deformation. In this dynamic environment the melts can segregate and eventually ascend [41,42,67]. Our model also does not take account of local interaction between intruding magmas and their host [21] and does not consider convective effects [2]. Dynamical processes will influence in detail the thermal profiles, melt compositions and evolution, and eventually can be incorporated into more advanced models. However, the large-scale findings of our models, i.e. incubation periods and the respective amounts of melts produced by crystallization of basalt and by crustal anatexis, are unlikely to be changed. The other dynamical processes only govern the details of how heat and volatiles are shared within the deep crustal intrusion zone. As one example escape of melt contemporaneously with the evolution of a deep crustal intrusion zone removes mass, but does not prevent further generation of melt. Melt removal does not remove significant enthalpy because: (i) as long as the melt fraction is low the heat is mostly stored in the solid fraction; (ii) in the basalt the melt is mostly accumulated by crystallization of new advected magma;

and (iii) the melt that would be extracted does not remove latent heat because as long as basalt intrusions proceed the system is moving toward more melting and less crystallization.

However compositional variations of melts and proportions of old and new crust in generated melts can be expected to change if different assumptions are made about melt segregation and fluid behavior. If melts are removed incrementally and continuously then the rocks in the deep hot zone will become more refractory and more difficult to melt with time. The amount of melt for a given addition of basalt intrusions is likely to be lower for a fractional melting model. For the wet basalt case some of the water may flux into overlying old crustal rocks and produce more melting than in our models. In cases were predicted proportions of melt exceed 25% dynamic processes must become important, because at high melt proportions the system is effectively a magma. Thus the model results with high degrees of melting are not likely to be correct in detail.

5. Conclusions

We have modelled the thermal evolution and melt generation caused by repeated intrusion of basalt into the deeper parts of the crust. The main controls on melt generation are magma intrusion rate, the composition and water content of the pre-existing crustal rocks, and the temperature and water content of the intruding basalt magma. For an initial geotherm below the solidus of the crust there is always an initial incubation period during which successive basalt intrusions completely solidify. However, for a range of magma intrusion rates thought to be representative of common tectonic situations, heat is advected into the zone of intrusion at a much faster rate than it can be conducted away. Consequently temperature increases and melting begins when the solidus is reached. The incubation period for a representative intrusion rate of a 50 m sill every 10 000 years at the boundary between the upper and lower crust ($\sim$20 km depth) is of order of hundreds of thousands of years. The incubation period is decreased for higher intrusion rates and for intrusion in deeper and hotter crust. For low intrusion rate conditions for melting of the crust may never occur. We estimate that magma intrusion rates of 50 m per 100 000 years or lower are not capable of causing crustal melting, but melt generation by crystallization of basalt at sub-Moho depths is possible.

Melt is generated simultaneously in a deep intrusion zone by cooling and crystallization of each increment of basalt intrusion and by partial melting of surrounding rocks due to heat transfer from invading basalt. Both older pre-existing crust and new basalt crust will contribute to the partial melts. The proportions of evolved melt generated from basalt differentiation, partial melting of new basalt crust and partial melting of old crust will strongly depend on lithology, in particular the proportions of hydrous minerals, and assumptions about the temperature and water content of the basalt magma. In the case of a wet cool basalt invading anhydrous infertile crust, as might for example occur in a continental arc with dry Pre-Cambrian crust, almost all the melt generated is derived by differentiation of newly emplaced basalt intrusions. In contrast large amounts of melting of old crust occur if hot dry basalt intrudes fertile crustal rocks, such as pelites. In almost all cases silicic melts generated by differentiation of basalt are significant contributions to melt generation. If the melts generated from such zones mix together during segregation then high-level silicic intrusions and volcanic products will be geochemical hybrids of mantle and crustal components. An implicit feature of all models of melt generation by intrusion of basalt into deep crustal intrusion zones is that a wide range of melt compositions is simultaneously generated. Thus such zones are likely to be a major cause of compositional diversity in magmas.

Deep crustal intrusion zones are long-lived thermal anomalies, which can take several million years to decay back to background geothermal gradients after magmatism is finished. Reverse geothermal gradients are a characteristic feature. If a new magmatic episode begins before the thermal anomaly has decayed then the earlier intruded zone is a preferential region for renewed partial melting.

Acknowledgements

We thank Jon Blundy, Chris Hawkesworth, Claude Jaupart and Daniel Vielzeuf for useful discussion. Reviews by Georges Bergantz and Nick Petford helped us to clarify the paper. The research was funded by a Swiss National Science Foundation grant (8220-64666) to C.A. and by a NERC Fellowship to R.S.J.S. *[AC]*

References

[1] W. Hildreth, Gradients in silicic magma chambers: implications for lithospheric magmatism, J. Geophys. Res. 86 (1981) 10153–10192.
[2] H.E. Huppert, R.S.J. Sparks, The generation of granitic magmas by intrusion of basalt into continental crust, J. Petrol. 29 (1988) 599–624.
[3] R.W. Kay, S. Mahlburg Kay, R.J. Arculus, Magma genesis and crustal processing, in: D.M. Fountain, R. Arculus, R.W. Kay (Eds.), Continental Lower Crust, Developments in Geotectonics vol. 23, Elsevier, Amsterdam, 1992, pp. 423–445.
[4] A.T. Anderson, Magma mixing: petrological process and volcanological tool, J. Volcanol. Geotherm. Res. 1 (1976) 3–33.
[5] J.C. Eichelberger, Andesitic volcanism and crustal evolution, Nature 275 (1978) 21–27.
[6] T. Furman, F.J. Spera, Co-mingling of acid and basic magma with implications for the origin of mafic I-type xenoliths: field and petrochemical relations of an unusual dike complex at Eagle Lake, Sequoia National Park, California, USA, J. Volcanol. Geotherm. Res. 24 (1985) 151–178.
[7] R.S.J. Sparks, L.A. Marshall, Thermal and mechanical constraints on mixing between mafic and silicic magmas, J. Volcanol. Geotherm. Res. 29 (1986) 99–124.
[8] C.R. Bacon, Magmatic inclusions in silicic and intermediate volcanic-rocks, J. Geophys. Res. 91 (1986) 6091–6112.
[9] J.D. Blundy, R.S.J. Sparks, Petrogenesis of mafic inclusions in granitoids of the Adamello Massif, Italy, J. Petrol. 33 (1992) 1039–1104.
[10] T. Koyaguchi, Evidence for two-stage mixing in magmatic inclusions and rhyolitic lava domes on Nijima Island, Japan, J. Volcanol. Geotherm. Res. 29 (1986) 71–98.
[11] R.H. Vernon, Crystallization and hybridism in microgranitoid enclave magmas: microstructural evidence, J. Geophys. Res. 95 (1990) 17849–17859.
[12] W.S. Holbrook, W.D. Mooney, N.I. Christensen, The seismic velocity structure of the deep continental crust, in: D.M. Fountain, R. Arculus, R.W. Kay (Eds.), Continental Lower Crust, Developments in Geotectonics vol. 23, Elsevier, Amsterdam, 1992, pp. 1–43.
[13] W. Franke, Phanerozoic structures and events in central Europe, in: D. Bundell, R. Freeman, S. Mueller (Eds.), A Continent Revealed. The European Geotraverse, Cambridge University Press, Cambridge, 1992, pp. 164–180.
[14] K. Fuchs, K.P. Bonjer, D. Gajewski, E. Lüschen, C. Prodehl, K.J. Sandmeier, F. Wenzel, H. Wilhelm, Crustal evolution of the Rhine graben area. 1. Exploring the lower crust in the Rhine graben rift by unified geophysical experiments, Tectonophysics 141 (1987) 261–275.
[15] F. Wenzel, J.P. Brun, A deep reflection seismic line across the Northern Rhine Graben, Earth Planet. Sci. Lett. 104 (1991) 140–150.
[16] G.Y. Bussod, D.R. Williams, Thermal and kinematic model of the southern Rio Grande rift inferences from crustal and mantle xenoliths from Kilbourne Hole, New Mexico, Tectonophysics 197 (1991) 373–389.
[17] J.P. Cull, S.Y. O'Reilly, W.L. Griffin, Xenolith geotherms and crustal models in Eastern Australia, Tectonophysics 192 (1991) 359–366.
[18] T.M. Brocher, Geometry and physical properties of the Sorroco, New Mexico, magma bodies, J. Geophys. Res. 86 (1981) 9420–9432.
[19] P.M. Sachs, T.H. Hansteen, Pleistocene underplating and metasomatism of the lower continental crust: a xenolith study, J. Petrol. 41 (2000) 331–356.
[20] M. Ducea, The California Arc thick granitic batholiths, eclogitic residues, lithospheric-scale thrusting, and magmatic flares-ups, GSA Today 11 (2001) 4–10.
[21] W. Hildreth, S. Moorbath, Crustal contribution to arc magmatism in the Andes of Central Chile, Contrib. Mineral. Petrol. 98 (1988) 455–489.
[22] J.E. Quick, S. Sinigoi, A. Mayer, Emplacement dynamics of a large mafic intrusion in the lower crust, Ivrea-Verbano Zone, northern Italy, J. Geophys. Res. 99 (1994) 21559–21573.
[23] S. Sinigoi, J. Quick, A. Mayer, G. Demarchi, Density-controlled assimilation of underplated crust, Ivrea-Verbano zone, Italy, Earth Planet. Sci. Lett. 129 (1995) 183–191.
[24] G. Rivalenti, G. Garuti, A. Rossi, F. Siena, S. Sinigoi, Existence of different peridotite types and of a layered igneous complex in the Ivrea Zone of the western Alps, J. Petrol. 22 (1981) 127–153.
[25] H.R. Shaw, Links between magma-tectonic rate balances, plutonism, and volcanism, J. Geophys. Res. 90 (1985) 11275–11288.
[26] P. Lipman, The roots of ash flow calderas in western North America: windows into the tops of granitic batholiths, J. Geophys. Res. 89 (1984) 8801–8841.
[27] R.A. Bailey, G.B. Dalrymple, M.A. Lanphere, Volcanism, structure, and geochronology of Long Valley Caldera, Mono County, California, J. Geophys. Res. 81 (1976) 725–744.
[28] T.H. Druitt, L. Edwards, R.M. Mellors, D.M. Pyle, R.S.J. Sparks, M. Lanphere, M. Davies, B. Barriero, Santorini Volcano, Geological Society Memoir 19, The Geological Society, London, 1999, 165 pp.
[29] M.P. Ryan, Elasticity and contractancy of hawaiian oliv-

ine tholeiite and its role in the stability and structural evolution of subcaldera magma reservoirs and rift systems, in: R.W. Decker, T.L. Wight, P.H. Stauffer (Eds.), Volcanism in Hawaii, U.S. Geological Survey Professional Paper 1350, 2, 1987, pp. 1395–1447.
[30] K. Putirka, Magma transport at Hawaii inferences based on igneous thermobarometry, Geology 25 (1997) 69–72.
[31] B.E. John, Structural reconstruction and zonation of a tilted mid-crustal magma chamber: the felsic Chemehuevi Mountains plutonic suite, Geology 16 (1988) 613–617.
[32] G.W. Bergantz, Underplating and partial melting: Implications for melt generation and extraction, Science 245 (1989) 1093–1095.
[33] N. Laube, J. Springer, Crustal melting by ponding of mafic magmas: a numerical model, J. Volcanol. Geotherm. Res. 81 (1998) 19–35.
[34] S.A. Barboza, G.W. Bergantz, Dynamic model of dehydration melting motivated by a natural analogue: applications to the Ivrea-Verbano zone, northern Italy, Trans. R. Soc. Edinburgh 87 (1996) 23–31.
[35] G.W. Bergantz, R. Dawes, Aspects of magma generation and ascent in continental lithosphere, in: M.P. Ryan (Ed.), Magmatic Systems, Academic Press, San Diego, CA, 1992, pp. 291–317.
[36] N. Petford, K. Gallagher, Partial melting of mafic (amphibolitic) lower crust by periodic influx of basaltic magma, Earth Planet. Sci. Lett. 5983 (2001) 1–17.
[37] D. McKenzie, D. Fairhead, Estimates of the effective elastic thickness of the continental lithosphere from Bouguer and free air gravity anomalies, J. Geophys. Res. 102 (1997) 27523–27552.
[38] D. Vielzeuf, J.R. Holloway, Experimental determination of the fluid-absent melting relations in the pelitic system, Contrib. Mineral. Petrol. 98 (1988) 257–276.
[39] A.E. Patino-Douce, A.D. Johnston, Phase equilibria and melt productivity in the pelitic system: implications for the origin of peraluminous granitoids and aluminous granulites, Contrib. Mineral. Petrol. 107 (1991) 202–218.
[40] K.P. Skjerlie, A.D. Johnston, Vapor-absent melting at 10 kbar of a biotite and amphibolite bearing gneiss: Implications for the generation of A-type granites, Geology 20 (1992) 263–266.
[41] D. McKenzie, The extraction of magma from the crust and mantle, Earth Planet. Sci. Lett. 74 (1985) 81–91.
[42] N. Petford, A.R. Cruden, K.J.W. McCaffrey, J.L. Vigneresse, Granite magma formation, transport and emplacement in the earth's crust, Nature 408 (2000) 669–673.
[43] J. deBremond d'Ars, C. Jaupart, R.S.J. Sparks, Distribution of volcanoes in active margins, J. Geophys. Res. 100 (1995) 20421–20432.
[44] J.L. Vigneresse, P. Barbey, M. Cuney, Rheological transitions during partial melting and crystallization with application to the felsic magma segregation and transfer, J. Petrol. 37 (1996) 1579–1600.
[45] J.D. Clemens, D. Vielzeuf, Constraints on melting and magma production in the crust, Earth Planet. Sci. Lett. 86 (1987) 287–306.
[46] B.O. Mysen, Melting curves of rock and viscosity of rock forming melts, in: Y.S. Touloukian, W.R. Judd, R.F. Roy (Eds.), Physical Properties of Rocks and Minerals, McGraw-Hill/CINDAS Data Series on Material Properties vol. II-2, 1981, pp. 361–407.
[47] T.H. Green, Anatexis of mafic crust and high pressure crystallization of andesite, in: Andesites: Orogenic Andesites and Related Rocks, Wiley, New York, 1982, pp. 465–487.
[48] P.J. Wyllie, Experimental studies on biotite- and muscovite-granites and some crustal magmatic sources, in: M.P. Atherton, C.D. Gribble (Eds.), Migmatites, Melting and Metamorphism, Shiva Publishing Limited, Cambridge, MA, 1983, pp. 12–26.
[49] J.D. Foden, D.H. Green, Possible role of amphibole in the origin of andesite: some experimental and natural evidence, Contrib. Mineral. Petrol. 109 (1992) 479–493.
[50] D.S. Chapman, K.P. Furlong, Thermal state of the continental lower crust, in: D.M. Fountain, R. Arculus, R.W. Kay (Eds.), Continental Lower Crust, Developments in Geotectonics vol. 23, Elsevier, Amsterdam, 1992, pp. 179–199.
[51] J.A. Crisp, Rates of magma emplacements and volcanic output, J. Volcanol. Geotherm. Res. 20 (1984) 177–211.
[52] H.A. Jelsma, M.L. Vinyu, P.J. Valbracht, G.R. Davies, J.R. Wijbrans, E.A.T. Verdurmen, Constraints on Archaean crustal evolution of the Zimbabwe Craton: a U-Pb Zircon, Sm-Nd and Pb-Pb whole-rock isotope study, Contrib. Mineral. Petrol. 124 (1996) 55–70.
[53] N. Petford, A.R. Cruden, K.J.W. McCaffrey, J.-L. Vigneresse, Granite magma formation, transport and emplacement in Earth's crust, Nature 408 (2000) 669–673.
[54] M. Haederle, M.P. Atherton, Shape and intrusion style of the Coastal Batholith, Peru, Tectonophysics 345 (2002) 17–28.
[55] T. Kawamoto, Experimental constraints on differentiation and H_2O abundance of calc-alkaline magmas, Earth Planet. Sci. Lett. 144 (1996) 577–589.
[56] J.S. Beard, G.E. Lofgren, Dehydration melting and water-saturated melting of basaltic and andesitic greenstones and amphibolites at 1, 3, and 6.9 kb, J. Petrol. 32 (1991) 365–401.
[57] G. Moore, I.S.E. Carmichael, The hydrous phase equilibria (to 3 kbar) of an andesite and basaltic andesite from western Mexico: constraints on water content and conditions of phenocryst growth, Contrib. Mineral. Petrol. 130 (1998) 304–319.
[58] D.S. Musselwhite, D.J. DePaolo, M. McCurry, The evolution of a silicic magma system: isotopic and chemical evidence from the Wods Mountains Volcanic Center, eastern California, Contrib. Mineral. Petrol. 101 (1989) 19–29.
[59] A. Soesoo, Fractional crystallization of mantle-derived melts as a mechanism for some I-type granite petrogenesis: an example from Lachlan Fold Belt, Australia, J. Geol. Soc. 157 (2000) 135–149.
[60] F. Wu, B. Jahn, S. Wilde, D. Sun, Phanerozoic crustal

growth: U-Pb and Sr-Nd isotopic evidence from the granites in northeastern China, Tectonophysics 328 (2000) 89–113.
[61] D.J. DePaolo, F.V. Perry, W.S. Baldridge, Crustal versus mantle sources of granitic magmas: a 2-parameter model based on Nd isotopic studies, Trans. R. Soc. Edinburgh 83 (1992) 439–446.
[62] J.W. Schlue, R.C. Aster, R.P. Meyer, A lower crustal extension to a midcrustal magma body in the Rio Grande Rift, New Mexico, J. Geophys. Res. 101 (1996) 25283–25291.
[63] B.R. Doe, W.P. Leeman, R.L. Christiansen, C.E. Hedge, Lead and strontium isotopes and related trace-elements as genetic tracers in the upper Cenozoic rhyolite-basalt association of the Yellowstone plateau volcanic field, J. Geophys. Res. 87 (1982) 4785–4806.
[64] J.M. Metz, G.A. Mahood, Precursors to the Bishop Tuff eruption: Glass Mountain, Long Valley, California, J. Geophys. Res. 90 (1985) 11121–11126.
[65] E. Cottrell, J.E. Gardner, M.J. Rutherford, Petrologic and experimental evidence for the movement and heating of the pre-eruptive Minoan rhyodacite (Santorini, Greece), Contrib. Mineral. Petrol. 135 (1999) 315–331.
[66] N. Petford, M.A. Koenders, Self-organisation and fracture connectivity in rapidly heated continental crust, J. Struct. Geol. 20 (1998) 1425–1434.
[67] J.D. Clemens, N. Petford, Granitic melt viscosity and silicic magma dynamics in contrasting tectonic settings, J. Geol. Soc. London 156 (1999) 1057–1060.
[68] W.A. Bohrson, F.J. Spera, Energy-constrained open-system magmatic processes II: application of energy-constrained assimilation-fractional crystallization (EC-AFC) model to magmatic systems, J. Petrol. 42 (2001) 1019–1041.
[69] B.S. Singer, J.D. Myers, S.R. Linnemann, C.L. Angevine, The thermal history of ascending magma diapirs and the thermal and physical evolution of magmatic conduits, J. Volcanol. Geotherm. Res. 37 (1989) 273–289.